EASR

Engineering and Applied Science Research

https://www.tci-thaijo.org/index.php/easr/index

Published by the Faculty of Engineering, Khon Kaen University, Thailand

Hexadecyltrimethylammonium-modified fly-ash zeolite for sulfate removal in treated coal-fired power plant effluent

Anyamanee Budput[1)], Dickson Y.S. Yan[2)], May Thu Than Htike[1)], Pummarin Khamdahsag[3)] and Visanu Tanboonchuy*[1, 4)]

[1)]Department of Environmental Engineering, Faculty of Engineering, Khon Kaen University, Khon Kaen 40002, Thailand
[2)]Faculty of Science & Technology, Technological and Higher Education Institute of Hong Kong, New Territories, Hong Kong
[3)]Environmental Research Institute, Chulalongkorn University, Bangkok 10330, Thailand
[4)]Research Center for Environmental and Hazardous Substance Management (EHSM), Khon Kaen University, Khon Kaen 40002, Thailand

Received 8 March 2023
Revised 23 June 2023
Accepted 26 June 2023

Abstract

This research was conducted primarily to examine sulfate ion (SO_4^{2-}) removal from aqueous solutions using zeolite NaP1 surface modified with hexadecyltrimethylammonium (HDTMA), or so-called MZ-HDTMA. To be suitable for SO_4^{2-} removal conditions, the synthetic conditions of MZ-HDTMA were optimized utilizing a Box-Behnken design approach. Experiments were conducted considering three factors that influence synthesis, including the amount of HDTMA cationic surfactant (3.33-6.67 wt%), mixing time (0.5-2 h), and drying temperature (50-80°C). The zeolite NaP1 synthesized from fly ash and MZ-HDTMA were characterized to compare their characteristics using techniques including point of zero charge (pH_{pzc}), scanning electron microscopy (SEM), and x-ray diffraction (XRD). The results from SO_4^{2-} removal showed that the most significant effect was the weight percentage of HDTMA. Adsorption kinetic studies revealed that modified zeolite had a SO_4^{2-} removal amount of 8.913 mg/g at equilibrium time and better fitted the pseudo-second-order model ($R^2 = 0.99$). This study established that more than 80% of the SO_4^{2-} in the aqueous solution was removed.

Keywords: Adsorption, Fly ash, Power plant, Sulfate, Zeolite

1. Introduction

Sulfate ion (SO_4^{2-}) is one of the contaminants caused by the discharge of industrial effluents. SO_4^{2-} ions are used as containers in the production of different chemicals, textiles, colors, soap, glass, paper, pesticides, and insecticides as well as in the pharmaceutical, metal, plating industries, wood pulp, and mining [1]. When SO_4^{2-} concentrations in aqueous solutions exceed 250 mg/L, it can cause corrosion in plumbing systems and a horrible taste in the water supply [2]. Concentrations in humans ranging between 500–750 mg/L result in gastrointestinal discomfort, catharsis, dehydration, and laxative action [2]. SO_4^{2-} in an aquatic environment mainly comes from industrial wastewater emissions, human activities, and oxidation processes for sulfur-containing minerals [3]. Industrial wastewater can come from acid mine drainage, dyeing, printing, and pharmaceutical wastewater. Particularly from coal-fired power plants, the SO_4^{2-} concentration in industrial effluents can reach several thousand milligrams per liter [4], while typical domestic effluent contains 20 to 500 mg/L of SO_4^{2-} [3]. In accordance with World Health Organization (WHO) and Environmental Protection Agency (EPA) guidelines, the standard value of SO_4^{2-} in drinking water must not exceed 250 mg/L, though it is recommended that the concentration should remain lower than 150 mg/L to prevent corrosion of water pipelines [2].

Many technologies are used for SO_4^{2-} removal such as biological treatment, chemical precipitation, adsorption, and electrodialysis. The innovative procedures of reverse osmosis and ion exchange can reduce effluent SO_4^{2-} concentration to less than 100 mg/L [5]. On the other hand, reverse osmosis filtering systems are costly, expensive to operate effectively, and require professional maintenance to ensure appropriate safety and functionality. Another disadvantage of reverse osmosis water filtration is that the efficacy of these systems to remove contaminants is not limited to only the harmful ones. Additionally, the pH of the treated water decreases by removing these minerals, making it more acidic. While this level of acidity is not harmful to people, the lower pH water is significantly more corrosive for plumbing systems, and it can cause lead and copper to be leached from pipes, which then dissolve into the water supply. Chemical precipitation does not completely remove SO_4^{2-} from water and produces sediment as a byproduct. Biological treatment can be SO_4^{2-} reduction due to the low volumes of sludge produced. However, the costs of biological treatment and ion exchange are high because of the long residence time requirement for biological treatment and the expensive cost of recovery after use for ion exchange. The disadvantage of electrodialysis is that it does not remove organic contaminants or microorganisms. Thus, post-treatment is required if high-quality water is necessary.

*Corresponding author.
Email address: visanu@kku.ac.th
doi: 10.14456/easr.2023.38

Adsorption is a method that has the potential to be employed in a hybrid system with precipitation. In such a system, the remaining SO_4^{2-} concentrations that are left over after the precipitation process could be eliminated using the adsorption process [6]. A vast number of materials with different characteristics have been evaluated as potential SO_4^{2-} adsorbents. For example, zeolite modification with barium was found to be an effective modification technique for SO_4^{2-} adsorption. Barium-modified analcime (ANA-Na-Ba) was the most effective sorbent material for the removal of SO_4^{2-}, having a maximum sorption uptake of 13.7 mg/g [7]. Malan loess is abundant in calcium and carbonate nodules, retains potent adsorption properties, and possesses a large surface area, high permeability, and high porosity. Similarly, it has a maximum sorption uptake of 123.86 mg/g [8]. Other natural SO_4^{2-} adsorbents include minerals that vary in efficacy for anion adsorption depending on their nature and characteristics. In mine waste rocks, Ni-Al metasomatic has a maximum sorption uptake of 53.07 mg/g [9].

SO_4^{2-} levels in coal-fired power plant effluent range between 20 and 500 mg/L [10]. In the process of preparing coal for burning, mining coal involves washing it with water and using chemicals to reduce contaminants such as sulfur and heavy metals. In this process, SO_4^{2-} contamination has been found in the wastewater. Further, the process of burning coal fuel to prevent air pollution from occurring means it is necessary to install a flue gas desulfurization system (FGD), which involves a reaction between flue gas and lime water or limestone either in the form of spraying or sprinkling. Added to the liquid, the reaction also results in the formation of sulfates or sulfides [11].

Consequently, zeolite has been an interesting option for processing the SO_4^{2-} removal procedure previously mentioned because there is a significant amount of waste in a coal-fired power plant and it should be reused. Furthermore, zeolite has high selectivity and porosity. It is also an environmentally friendly and inexpensive chemical [10, 12]. Such a zeolite/cerium oxide coat on an activated alumina ball could increase the efficiency of arsenite removal [13]. Selenate can be removed using zeolite NaP1-supported nanoscale zero-valent iron (Z-NZVI) [14]. Likewise, it is well known that quaternary amine-modified zeolite may significantly improve the anionic adsorption from aqueous solutions. According to earlier research, zeolite from coal fly ash that has been treated with surfactants works well as an adsorbent to remove chromate anions. The maximum adsorption capacities were 11.268 and 1.938 mg/g for modified clinoptilolite and modified Linde Type A zeolite, respectively [15].

In their molecular structures, these quaternary amines consist of a hydrophilic, positively charged head group and a hydrophobic tail. Hexadecyltrimethylammonium (HDTMA) is one of the most frequently used surfactants for zeolite surface modification because of its high efficacy [16].

This paper compares the performance of synthesized zeolite NaP1 and modified zeolite in the aqueous SO_4^{2-} adsorption process. Modified zeolites have previously been subjected to surface conditioning with HDTMA surfactant, namely MZ-HDTMA. The effects of concentration, mixing time, and temperature in the dry oven were studied analytically using the Box-Behnken design. The ability of MZ-HDTMA to remove SO_4^{2-} from each condition was then tested. The adsorption kinetics models were calculated, while the crystallinity, point of zero charges (pH_{pzc}), and morphology of the synthesized zeolite NaP1 and MZ-HDTMA were characterized.

2. Materials and methods

2.1 Chemicals

The fly ash used in this experiment was collected from a coal-fired power plant in Lampang Province, Thailand. The chemicals used in this study were sodium sulfate anhydrous (Na_2SO_4, 99%) (RCL Labscan, Thailand), hexadecyltrimethylammonium bromide (HDTMA, 100%) (Sigma-Aldrich, Singapore), sodium hydroxide (NaOH, 99%) (RCL Labscan, Thailand), and deionized water.

2.2 Synthesis of zeolite NaP1 and MZ-HDTMA

The zeolite NaP1 synthesis was prepared using the following procedure [10]. Firstly, solution A was prepared by dissolving 8.27 g of NaOH in deionized water, mixing 7.98 g of fly ash, and stirring at 100°C. Solution B involved dissolving 10 g of NaOH in deionized water, mixing 16.86 g of fly ash, and stirring at 100°C. Subsequently, 5.61 g of NaOH was added to 10 g of solution B. Afterwards, during the following 30 min, solutions A and B were mixed completely. After that, the combined solution was put into a stainless steel autoclave with Teflon lining before spending 12 h in a 100°C oven. The solution was then separated using a centrifugal method. The material was separated from the supernatant liquid, rinsed with deionized water until the pH was less than 9.0, and then dried for 24 h at 100°C in an oven. Finally, the synthesized zeolite NaP1 from the fly ash was obtained.

To synthesize MZ-HDTMA, the HDTMA solution was prepared by dissolving an appropriate amount of HDTMA in 50 mL of deionized water and stirring gently until all HDTMA was dissolved. After that, the HDTMA solution was mixed with the synthesized zeolite NaP1 and the mixture was stirred at room temperature, end-over-end stirred, and dried following experiments by the Box-Behnken design. Data analysis was carried out with Design Expert® software version 7, applying response surface methodology with Box-Behnken design. The effects of three variables were studied, including the weight percentage of HDTMA (X_1), mixing time (X_2), and drying temperature (X_3). In this work, 15 experiments were carried out for the MZ-HDTMA (Table 1).

Table 1 Levels of independent variables for MZ-HDTMA

Level	Representative	Level of parameter		
		Low	Medium	High
HDTMA (wt%)	X_1	3.33	5.00	6.67
Mixing time (h)	X_2	0.5	1.25	2
Drying temperature (°C)	X_3	50	65	80

Both synthesized zeolite NaP1 and MZ-HDTMA were characterized using an X-ray diffractometer (XRD) (D8 Discover, Bruker AXS) with Cu Kα radiation (λ = 0.1514 nm) at 40 mA and 40 kV. The scan range was between 10-80° with an increment of 0.02°/step. The areas, peak positions, and widths were estimated using ORIGIN®8.5. The point of zero charges (pHpzc) was determined according to a previously recommended method [17]. Their morphology was analyzed using a scanning electron microscope (SEM, 1450VP, LEO).

2.3 Characterization of materials

The chemical composition and crystallographic structure were determined by X-ray diffraction (XRD, Bruker D8 Advance; Germany) with CuKα radiation (40 kV, 40 mA). The XRD patterns of materials were measured in a range of 2 Theta = 10–50°, with an increment of 0.02°/step, and a scan speed of 0.1 s/step at 298 K. The surface morphology was characterized by Field Emission Scanning Electron Microscopy (FE-SEM) (Carl Zeiss Model Auriga; Germany). The specific surface area of the samples was determined using the Brunauer-Emmett-Teller method at 77 K on a Bel Sorp mini II specific surface area and pore size distribution analyzer (Japan).

The zero point charge (pH_{zpc}) was determined by adding 0.01 M NaCl as an electrolyte and 0.1 M HCl or 0.1 M NaOH as a pH-adjusting agent. A total of 50 mL of electrolyte was poured into 6 Erlenmeyer flasks, and the solution pH was adjusted from 2 to 10. Zeolite NaP1 (0.5 g) was added to each flask, after which the flask was agitated for 48 h. Next, the zeolite NaP1 was separated by filtration and the final pH of the filtrate was determined. By plotting the initial pH value versus the ΔpH value (final pH - initial pH), it is possible to calculate the pHzpc of zeolite NaP1 from the intersection of such a plot [16].

2.4 Batch adsorption

2.4.1 Kinetic studies

The adsorption of SO_4^{2-} on synthesized zeolite NaP1 and MZ-HDTMA was carried out using the batch method. SO_4^{2-} uptake experiments were carried out using Na_2SO_4 solutions. An accurate amount of MZ-HDTMA (3 g) was added to a Na_2SO_4 solution (1 L) at a concentration of 50 ppm. The mixtures were shaken at an agitation rate of 300 rpm for 60 minutes. The mixture was then filtered, and the filtrate was analyzed for SO_4^{2-} concentration by UV-vis spectrophotometry (Turbidimetric method).

Reagent buffer solution A was dissolved 30 g of magnesium chloride ($MgCl_2 \cdot 6H_2O$), 5 g of sodium acetate ($CH_3COONa \cdot 3H_2O$), 1 g of potassium nitrate (KNO_3), and 20 mL of acetic acid (CH3COOH (99%)), in 500 mL deionized water and make up to 1000 mL. The sample was then mixed with buffer solution A and 20 to 30 meshes of barium chloride ($BaCl_2$) was stirred at a constant speed for exactly 1 min. After that, wait 5 min before analyzing the sample with UV-vis spectrophotometry at 420 nm and a light path of 2.5-10 cm (4500-SO_4^{2-} SULFATE - Standard Methods for the Examination of Water and Wastewater, n.d.).

The removal efficiency of SO_4^{2-} was calculated as follows:

$$R(\%) = ((C_0 - C_t)/C_0) \times 100 \quad (1)$$

where R is the percentage of SO_4^{2-} removed, C_0 and C_t are SO_4^{2-} at an initial concentration (50 ppm) and concentration following the reaction time, respectively. Pseudo-first-order and pseudo-second-order equations were applied to characterize the adsorption kinetic behavior of SO_4^{2-} removal efficacy and were compared between synthesized zeolite NaP1 and MZ-HDTMA. They were calculated as follows:

$$\ln q_e - q_t = \ln q_e - k_1 t \quad (2)$$

$$t/q_t = 1/(k_2 q_e^2) + t/q_e \quad (3)$$

where q_e and q_t are the amounts of SO_4^{2-} removal at equilibrium and time t (mg/g), k_1 and k_2 are the equilibrium rate constant of pseudo-first-order kinetics (min^{-1}), and pseudo-second-order kinetics (g·mg/min), respectively.

3. Results and discussion

3.1 Material characterization

The X-ray diffraction (XRD) patterns of synthesized zeolite NaP1 and MZ-HDTMA are shown in Figure 1(a). The XRD analysis confirmed that the formation of MZ-HDTMA did not change the phase of the synthesized zeolite NaP1. The results demonstrated that the primary phases found in both synthesized zeolite NaP1 ($Na_6Al_6Si_{10}O_{32}12H_2O$) and MZ-HDTMA following the JCPDS 39-0219 standard were mullite ($Al_2Si_2O_{13}$) and a minuscule amount of quartz (SiO_2) [18, 19].

The surface charges of synthesized zeolite NaP1 and MZ-HDTMA were revealed by pH_{pzc} measurements. When the solution pH was below $pH_{pzc,}$ the surface charges of materials became more positive, whereas, in the pH solution above pH_{pzc}, the surface of the material was negatively charged as presented [17]. Figure 1(b) reveals that the pH_{pzc} of the synthesized zeolite NaP1 is 10.3, while MZ-HDTMA is 8.9. This implies that the modification of zeolite by HDTMA can increase the positive charge on synthesized zeolite NaP1.

SEM images of synthesized zeolite NaP1 and MZ-HDTMA are shown in Figures 1(c) and 1(d), respectively. The surface of synthesized zeolite NaP1 has a smooth structure, although with the formation of sodium-silicate and alumino-silicate structures [14]. Also, it can be seen that the average particle size of synthesized zeolite NaP1 was 25 μm. MZ-HDTMA is somewhat larger than synthesized zeolite NaP1, although its average size is 105 μm, and most of its particles (80%) are located below 120 μm.

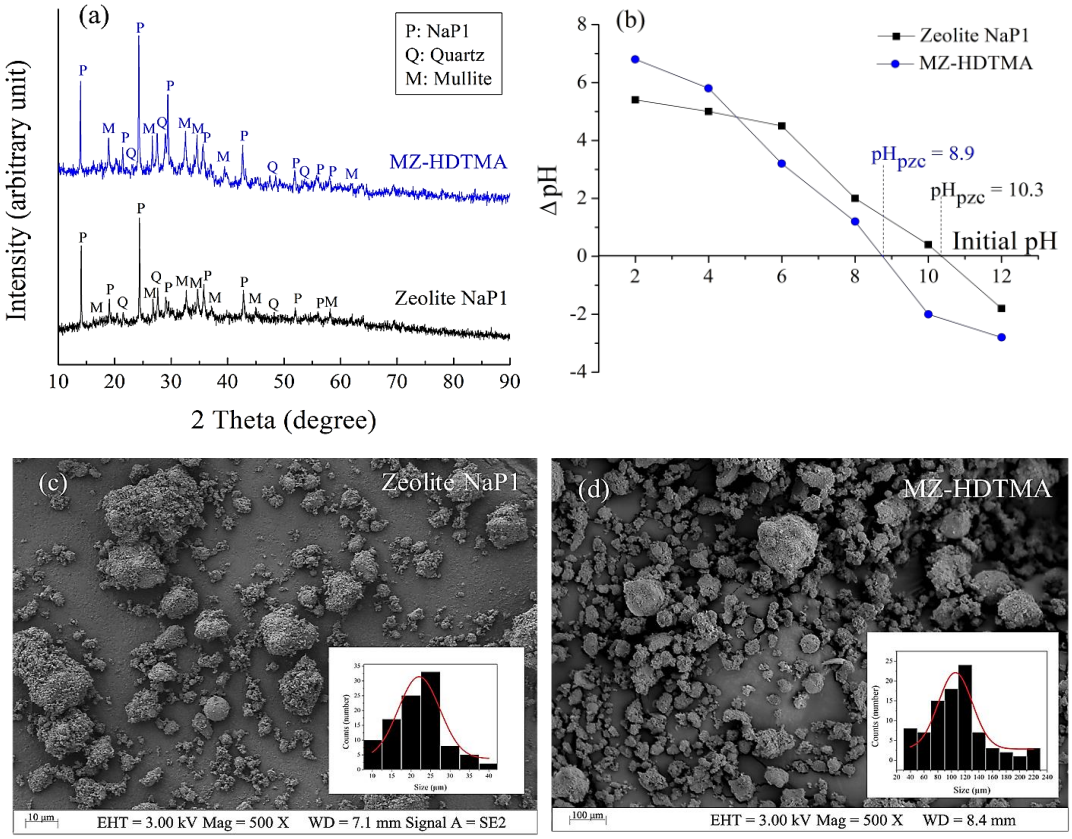

Figure 1 Characteristics of synthesized zeolite NaP1 and MZ-HDTMA from (a) XRD patterns, (b) point of zero charge plots, and (c) and (d) SEM images with inset plots of particle size distribution

3.2 Statistical analysis

The data points on the normal probability plot shown in Figure 2(a) were quite near a straight line, indicating that there were no obvious problems with normality. Figure 2(b) shows the internal standardized residual plots against the number that best fits the data. The plot shows a random scatter, which shows that the differences between the original readings are the same for all answer values. The histogram chart shown in Figure 2)c) demonstrates that the frequency of standardized residual was distributed in the normality of the curve. Figure 2(d) shows a plot of standardized residual versus batch runs of SO_4^{2-} removal and a plot of standardized residual versus run order. The results show random scatters that move around the center line in the plots of stand residual. These findings demonstrated the random distribution of the data. As displayed, the data were reliable and accurate. It has been explained that there was no anomaly in the observation order for the experiment orders. Thus, it can be said that the regression model served a purpose in identifying the important parameters as well.

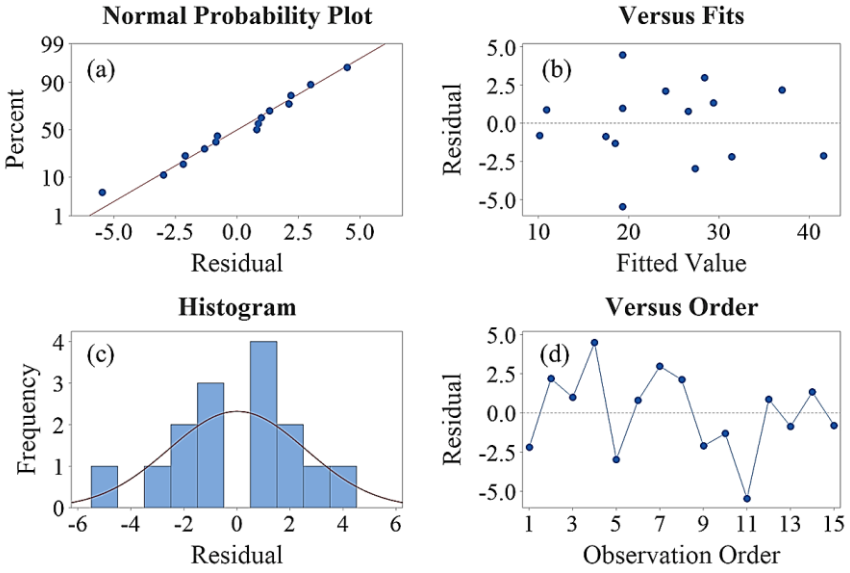

Figure 2 Internal standardized residual plots versus (a) normal probability, (b) fit, (c) histogram, and (d) observation order for percent removal of SO_4^{2-} at 60 min

Table 2 Estimated regression coefficients for predicting SO_4^{2-} removal efficiency

Term	Parameter	Coefficient	P-value
Constant		19.32	0.001
HDTMA (wt%)	X_1	5.79	0.013
Mixing time (h)	X_2	-2.48	0.166
Drying temperature (°C)	X_3	2.98	0.109
HDTMA (wt%) * HDTMA (%wt)	X_1*X_1	2.27	0.358
Mixing time (h) * Mixing time (h)	X_2*X_2	-5.32	0.064
Drying Temp (°C) * Drying Temp (°C)	X_3*X_3	11.91	0.003
HDTMA (wt%) * Mixing time (h)	X_1*X_2	-2.10	0.376
HDTMA (wt%) * Drying temperature (°C)	X_1*X_3	-0.68	0.766
Mixing time (h) * Drying temperature (°C)	X_2*X_3	1.97	0.404
Lack-of-Fit			0.693
R^2 = 92.19% R(adj) = 78.14%			

The MZ-HDTMA under various synthesized conditions through SO_4^{2-} removal is shown in Table 2. The coefficient values can be used to predict the percentage of SO_4^{2-} removal, as displayed in Equation (4). A positive sign in front of each parameter indicates a synergistic effect, while a negative sign implies an antagonistic effect. Moreover, the results shown in Table 2 reveal that the dominant effect on SO_4^{2-} removal was the weight percentage of HDTMA and the lack-of-fit value was 0.693, a value assessed at a significance level (α) of greater than 0.05 using a regression model.

$$Y = 217.5 - 0.8X_1 + 17.4X_2 - 6.77X_3 + 0.816X_1 * X_1 - 9.46X_2 * X_2 + 0.05294X_3 * X_3 - 1.68X_1 * X_2 - 0.0271X_1 * X_3 + 0.175X_2 * X_3 \quad (4)$$

In the equation, Y represents the percentage of SO_4^{2-} removal. Figure 3 and Table 3 shows the relationship between the predicted and experimental values from the model calculated by Eq. 4. The obtained data points were very close to linear (R^2 = 0.92), indicating that both values were accurate and reliable.

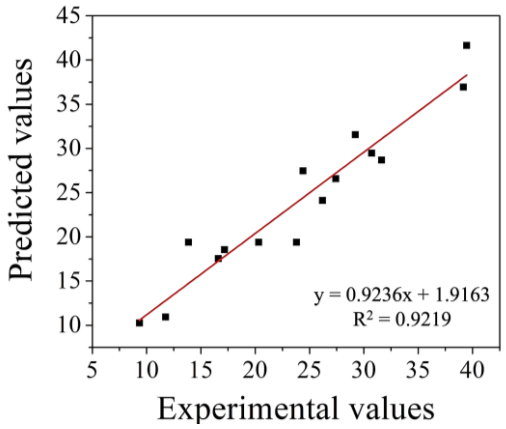

Figure 3 Plot of predicted values and experimental values for sulfate removal efficiency

Table 3 Experimental design matrix and comparison of the experimental data with sulfate removal to the predicted values obtained from the Box-Behnken design

Run No.	Independent variable			Sulfate removal (%)	
	HDTMA (wt%), X_1	Mixing time (h), X_2	Drying temperature (°C), X_3	Experimental data	Predicted value
1	3.33	1.25	80	29.22	31.36
2	6.67	1.25	50	39.16	37.18
3	5	1.25	65	20.31	19.40
4	5	1.25	65	23.80	19.40
5	5	0.5	50	24.40	27.49
6	6.67	0.5	65	27.41	26.76
7	5	2	80	31.36	28.44
8	3.33	1.25	50	26.20	24.14
9	6.67	1.25	80	39.46	41.68
10	5	2	50	17.17	18.64
11	5	1.25	65	13.86	19.40
12	3.33	0.5	65	11.75	10.87
13	6.67	2	65	16.60	17.64
14	5	0.5	80	30.72	29.41
15	3.33	2	65	9.34	10.16
			S.D. (%)	11.99	

3.3 Effect of independent variables on sulfate removal

Contour and surface plots were used to understand the influence of the independent variables. Figure 4 displays the correlation between the percentage of SO_4^{2-} removed and the independent parameters. The optimization conditions were analyzed by the Box-Behnken design. MZ-HDTMA synthesis conditions provided the highest percentage of SO_4^{2-} removal with 6.67 wt% of HDTMA, 1.25 h of mixing time, and 80°C of drying temperature.

The contour and surface plots in Figure 5 show the primary influences of the independent factors on SO_4^{2-} elimination. For the effect of weight percentage for HDTMA (3.33, 5, and 6.67), high removal was observed at a high weight percentage. The adsorption of SO_4^{2-} on the surface of the MZ-HDTMA is attributed to the formation of a bilayer at its surface. The hydrophobic surfactant chains cause an inversion of the surface charge on the zeolite during the creation of the bilayer, resulting in places where the anions can be exchanged. For the hydrophobic side of surfactants, they form micelles to avoid exposure to water. Surfactant molecules, in particular, are concentrated in their contact solutions, where they direct the hydrophilic group inward and the hydrophobic group outward. Micelles are not identifiable in highly diluted solutions or at low surfactant concentrations [15, 20].

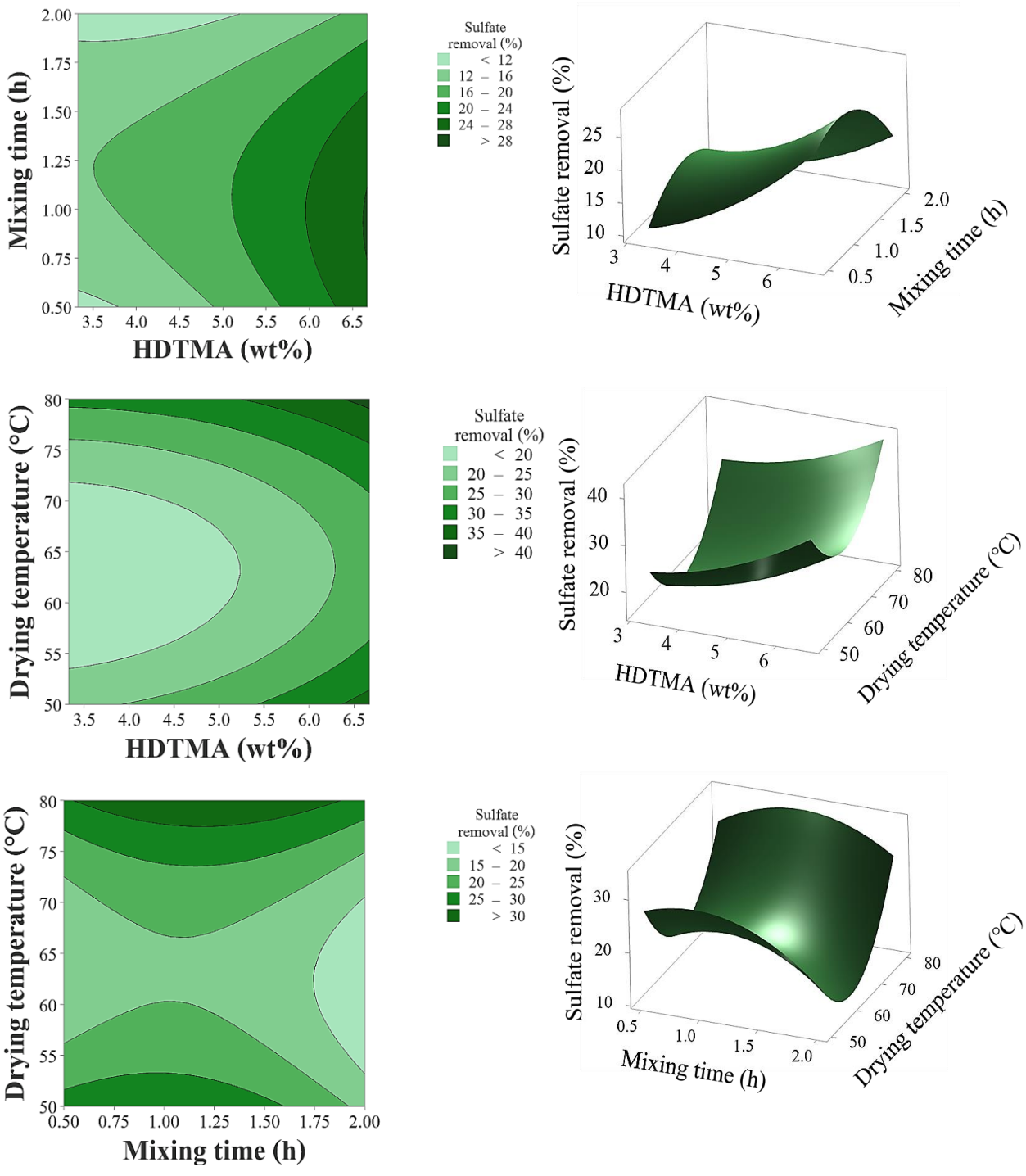

Figure 4 Contour plots and surface plots of sulfate removal efficiency

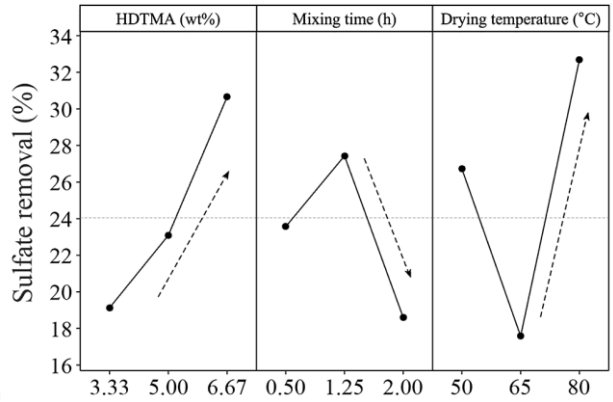

Figure 5 Plots of the main effects including the weight percentage of HDTMA (X_1), mixing time (X_2), and drying temperature (X_3) on sulfate removal

3.4 Adsorption kinetics of sulfate removal over synthesized zeolite NaP1 and MZ-HDTMA

The adsorption kinetics studies of sulfate removal over synthesized zeolite NaP1 and MZ-HDTMA were investigated for comparison, as shown in Figure 6. The conditions for MZ-HDTMA included a 6.67 wt% of HDTMA, a mixing time of 1.25 h, and a temperature of 80°C for a dry oven. The study results showed that the efficiency for removing SO_4^{2-} at 40 min of zeolite NaP1 and MZ-HDTMA were 5 and 80%, respectively. The potential rate of reaction was determined by pseudo-first-order and pseudo-second-order kinetics models (Table 4). In this model, K_1 is the equilibrium constant for the pseudo-first-order and K_2 is the equilibrium constant for the pseudo-second-order. The pseudo-first-order model produced much lower values for the correlation coefficient (R^2) than when the pseudo-second-order model was used. Moreover, the amount of SO_4^{2-} removal at equilibrium time for the MZ-HDTMA (8.913 mg/g) was slightly higher than that of synthesized zeolite NaP1 (0.271 mg/g). Therefore, the pseudo-second-order model indicated an adsorption process that was rate controlled for SO_4^{2-} removal by synthesized zeolite NaP1 and MZ-HDTMA. The results of intraparticle diffusion for SO_4^{2-} ion adsorption into the synthesized zeolite NaP1 and MZ-HDTMA. Plotting q_t versus $t^{0.5}$ presents a straight line that passes via the starting point, which demonstrates that the only step that may regulate the rate is intraparticle diffusion. The slope of each linear segment in the plot is used to precisely calculate the rate of adsorption; a steeper slope indicates a more rapid adsorption process [21]. In MZ-HDTMA, the diffusion rate constants for external (k_{i1}) and internal (k_{i2}) mass transfer were found to be 0.22 and 0.031 mg/g·min$^{1/2}$, respectively.

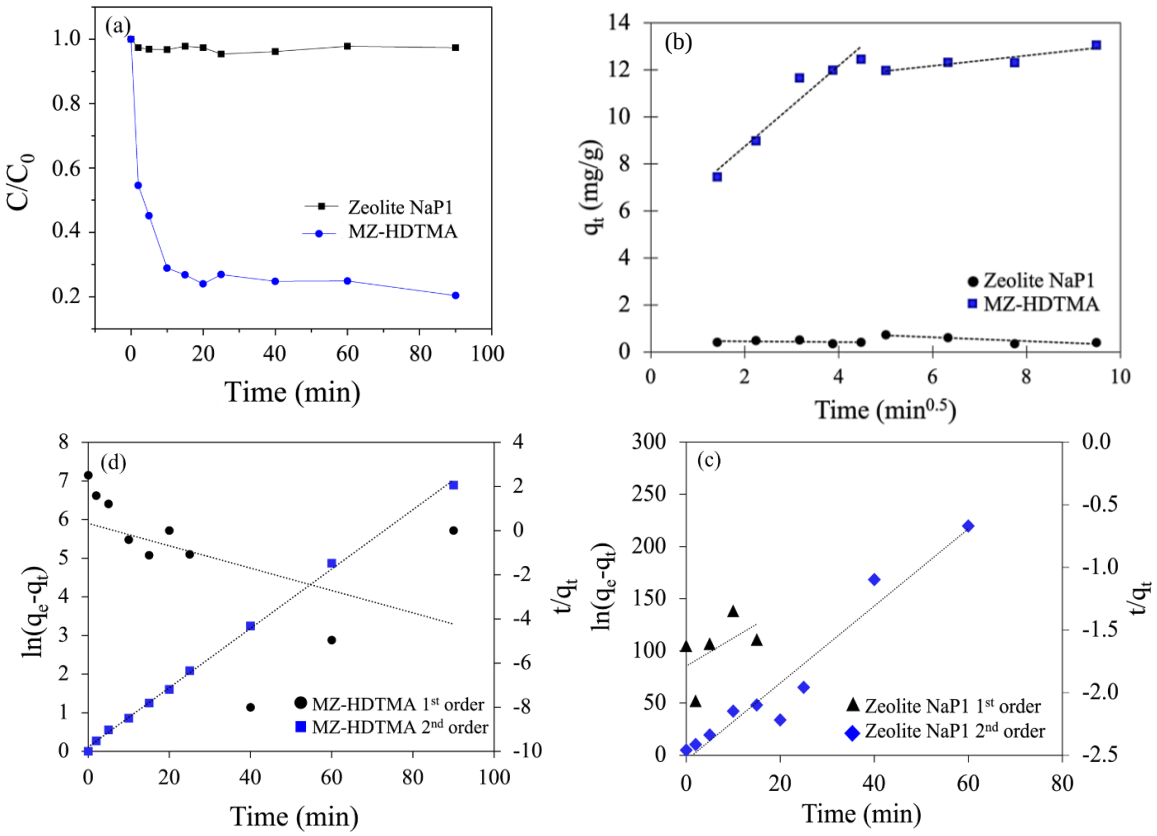

Figure 6 (a) Kinetic parameters for sulfate ions on synthesized zeolite NaP1 and MZ-HDTMA showing the concentration of sulfate ion a period of time, (b) the pseudo-first-order and pseudo-second-order kinetics models, and (c) and (d) intraparticle diffusion (experimental conditions: [SO_4^{2-}] = 50 ppm, Synthesized zeolite NaP1 = 3 g/L, and MZ-HDTMA = 3 g/L)

Table 4 Calculated parameters of adsorption kinetics for sulfate adsorption on synthesized zeolite NaP1 and MZ-HDTMA

Kinetics model	Parameter	Material	
		Zeolite NaP1	MZ-HDTMA
Pseudo-first-order	q_e(exp) (mg/g)	0.617	12.327
	q_e (mg/g)	5.981	3.469
	K_1 (min^{-1})	0.022	0.189
	R^2	0.28	0.81
Pseudo-second-order	q_e(exp) (mg/g)	0.617	12.327
	q_e (mg/g)	0.271	8.913
	K_2 ($g/mg \cdot min^{-1}$)	0.1605	2.927
	R^2	0.94	0.99
Intraparticle	K_{i1} ($mg/g \cdot min^{1/2}$)	0.0077	0.22
	R^2	0.33	0.52
	K_{i2} ($mg/g \cdot min^{1/2}$)	0.0073	0.031
	R^2	0.45	0.83

4. Conclusions

MZ-HDTMA-modified zeolite NaP1 was used to remove sulfate ions (SO_4^{2-}) from aqueous solutions. The results of SO_4^{2-} removal by MZ-HDTMA from the Box-Behnken design showed that the optimal conditions included a 6.67 weight percentage of HDTMA, a mixing time of 1.25 h, and a dry oven temperature of 80˚C. Further, the variable that had the greatest effect on SO_4^{2-} removal was the weight percentage of HDTMA. According to the findings of a kinetic investigation, the reaction rate of MZ-HDTMA was best represented by a pseudo-second-order model. Furthermore, the quantity of SO_4^{2-} removal at equilibrium time for the MZ-HDTMA was found to be 8.913 mg/g. Thus, the synthesized zeolite NaP1 from coal fly ash treated with HDTMA could potentially be used as a sorbent to remove SO_4^{2-} from water.

5. Acknowledgements

This work received funding support from the Fundamental Fund (the National Science, Research, and Innovation Fund (NSRF), Thailand) and the Faculty of Engineering, Khon Kaen University (Grant No. M-Eng.-ENVI-002/2564).

6. Reference

[1] Greenwood NN, Earnshaw A. Chemistry of the Elements. New York: Pergamon Press; 1984.
[2] US EPA. Sulfate in Drinking Water [Internet]. 2012 [cited 2022 Oct 23]. Available form: https://archive.epa.gov/water/archive/web/html/sulfate.html.
[3] Lens PNL, Visser A, Janssen AJH, Hulshoff Pol LW, Lettinga G. Critical reviews in environmental science and technology biotechnological treatment of sulfate-rich wastewaters biotechnological treatment of sulfate-rich wastewaters. Crit Rev Environ Sci Technol. 1998;28(1):41-88.
[4] Zhang J, Tang L, Zhang H, Yang Y, Mao Z. A novel and cleaner technological process of extracting l-glutamic acid from fermentation broth by two-stage crystallization. J Clean Prod. 2012;20(1):137-44.
[5] Sadeghalvad B, Khorshidi N, Azadmehr A, Sillanpää M. Sorption, mechanism, and behavior of sulfate on various adsorbents: a critical review. Chemosphere. 2021;263:128064.
[6] Runtti H, Tuomikoski S, Kangas T, Kuokkanen T, Rämö J, Lassi U. Sulphate removal from water by carbon residue from biomass gasification: Effect of chemical modification methods on sulphate removal efficiency. BioRes. 2016;11(2):3136-52.
[7] Runtti H, Tynjälä P, Tuomikoski S, Kangas T, Hu T, Rämö J, et al. Utilisation of barium-modified analcime in sulphate removal: isotherms, kinetics and thermodynamics studies. J Water Process Eng. 2017;16:319-28.
[8] Zheng Q, Zhang Y, Li Y, Zhang Z, Wu A, Shi H. Adsorption of sulfate from acid mine drainage in Northwestern China using Malan loess. Arab J Geosci. 2019;12(11):348.
[9] Sadeghalvad B, Azadmehr A, Hezarkhani A. A new approach to improve sulfate uptake from contaminated aqueous solution: metal layered double hydroxides functionalized metasomatic rock. 2019;54(4):447-66.
[10] Phanthasri J, Grisdanurak N, Khamdahsag P, Wantala K, Khunphonoi R, Wannapaiboon S, et al. Role of zeolite-supported nanoscale zero-valent iron in selenate removal. Water Air Soil Pollut. 2020;231(5):199.
[11] Córdoba P. Status of flue gas desulphurisation (FGD) systems from coal-fired power plants: overview of the physic-chemical control processes of wet limestone FGDs. Fuel. 2015;144:274-86.
[12] Suwannatrai S, Yan DYS, Phanthasri J, Khamdahsag P, Wannapaiboon S, Tanboonchuy V. Oxidation–adsorption of arsenite contaminated water over ceria nanorods. Desalin Water Treat. 2020;200:252-61.
[13] Suwannatrai S, Yan DYS, Khamdahsag P, Tanboonchuy V. Zeolite/Cerium oxide coat-on activated alumina ball for arsenite removal via fixed- bed continuous flow adsorption column. Appl Sci Eng Prog. 2022;15(4):1-10.
[14] Phanthasri J, Yan DYS, Wantala K, Khunphonoi R, Tanboonchuy V. Reduction and adsorption co-processes for selenate removal by zeolite-supported nanoscale zero-valent iron. Eng Applied Sci Res. 2022;49(3):363-72.
[15] Dimas Rivera GL, Martínez Hernández A, Pérez Cabello AF, Rivas Barragán EL, Liñán Montes A, Flores Escamilla GA, et al. Removal of chromate anions and immobilization using surfactant-modified zeolites. J Water Process Eng. 2021;39:101717.
[16] Łach M, Grela A, Pławecka K, Guigou MD, Mikuła J, Komar N, et al. Surface modification of synthetic zeolites with Ca and HDTMA compounds with determination of their phytoavailability and comparison of CEC and AEC parameters. Materials. 2022;15(12):4083.
[17] Noroozi R, Al-Musawi TJ, Kazemian H, Kalhori EM, Zarrabi M. Removal of cyanide using surface-modified Linde Type-A zeolite nanoparticles as an efficient and eco-friendly material. J Water Process Eng. 2018;21:44-51.

[18] Izidoro JDC, Fungaro DA, dos Santos FS, Wang S. Characteristics of Brazilian coal fly ashes and their synthesized zeolites. Fuel Process Technol. 2012;97:38-44.
[19] Szala B, Bajda T, Matusik J, Zięba K, Kijak B. BTX sorption on Na-P1 organo-zeolite as a process controlled by the amount of adsorbed HDTMA. Microporous Mesoporous Mater. 2015;202:115-23.
[20] de Gennaro B. Chapter 3 - Surface modification of zeolites for environmental applications. In: Mercurio M, Sarkar B, Langella A, editors. Modified Clay and Zeolite Nanocomposite Materials: Environmental and Pharmaceutical Applications. Amsterdam: Elsevier Inc; 2018. p. 57-85.
[21] Huang Y, Lee X, Grattieri M, Macazo FC, Cai R, Minteer SD. A sustainable adsorbent for phosphate removal: modifying multi-walled carbon nanotubes with chitosan. J Mater Sci. 2018;53(17):12641-9.